

The remarkably high excitation planetary nebula GC 6537

LAWRENCE H. ALLER^{†‡}, SIEK HUNG^{‡§}, AND WALTER A. FEIBELMAN^{‡¶}

[†]Physics and Astronomy Department, University of California, Los Angeles, CA 90095; [§]Bohyunsan Optical Observatory, Jachun P.O. Box 1, Youngcheon, Kyungbuk 770-820, South Korea; [¶]Laboratory for Astronomy and Solar Physics, Code 681, National Aeronautics and Space Administration Goddard Space Flight Center, Greenbelt, MD 20771

Contributed by Lawrence H. Aller, March 19, 1999

ABSTRACT NGC 6537 is an unusually high excitation point symmetric planetary nebula with a rich spectrum. Its kinematical structures are of special interest. We are here primarily concerned with the high resolution spectrum as revealed by the Hamilton echelle Spectrograph at Lick Observatory (resolution $\approx 0.2 \text{ \AA}$) and supplemented by UV and near-UV data. These extensive data permit a determination of interstellar extinction, plasma diagnostics, and ionic concentrations. The photoionization models that have been used successfully for many planetary nebulae are not entirely satisfactory here. The plasma electron temperature of a photoionization model cannot much exceed 20,000 K, but plasma diagnostics show that regions emitting radiation of highly ionized atoms such as [NeIV] and [NeV] are much hotter, showing that shock excitation must be important, as suggested by the remarkable kinematics of this object. Hence, instead of employing a strict photoionization model, we are guided by the nebular diagnostics, which reveal how electron temperature varies with ionization potential and accommodates density effects. The predictions of the photoionization model may be useful in estimating ionization correction factor. In effect, we have estimated the chemical composition by using both photoionization and shock considerations.

At nearly the final stage of a star's life, it has developed a small, dense, hot core surrounded by a vast tenuous envelope. Depending on its mass, it is then a giant or super giant. The envelope is subsequently ejected often to form a planetary nebula (PN). Such nebulae are rarely spherically symmetrical; often they are filamentary, with an inhomogeneous shell structure. Often they are bipolar or bilaterally symmetrical. The proto-PN are usually optically invisible. As the rapidly thinning shell becomes exposed to the radiation from the uncovered core, it becomes photoionized. Recombination of ions and electrons and collisional excitation of low lying levels produces the visible radiation of the PN. In kinematically active objects, shocks may also serve to heat the gas to incandescence.

Two of the highest excitation PN known are NGC 6302 and NGC 6537, in which also shock heating is very important (1–3). Both are probably extreme examples of Peimbert's type I (4), of which the prototype is NGC 2440. They originate from short-lived stars much more massive than the sun, perhaps 5–6 solar masses. Yet more massive stars are believed to eventually evolve into neutron stars and supernovae.

NGC 6537 exhibits a huge excitation range from [Ni] to [SiVI]1, i.e., from neutral atoms to ions requiring an ionization energy of 167 eV ($1 \text{ eV} = 1.602 \times 10^{-19} \text{ J}$). Ashley and Hyland (1) derive an upper limit to the stellar temperature of 240,000 K as compared with a Zanstra HeII T^* = 150,000 K and a model T^* = 180,000 K.

Various studies of NGC 6537 have elucidated its fascinating kinematical and topological structure (5–7). There is a bright inner core of $\approx 10^7$ diameter, whose spectroscopic properties

constitute the subject of this paper. The central density is $N_e = 20,000/\text{cc}$, falling off to $\approx 1,000/\text{cc}$ at the edge of the bright portion and finally to $\approx 200/\text{cc}$ at the outermost luminous edges. The electron temperature, T_e , varies from 6,000 to 47,000. The density also varies.

The complex structure of the outer nebulosity is distinguished by its complicated kinematics. There seems to be a wind of $\approx 18 \text{ km/sec}$ associated with dense blobs in the core, co-spatial with a fast wind with a velocity of 4,400 km/sec (7). Corradi and Schwarz (5) found the deprojected expansion polar velocity to be 300 km/sec. Thus, the initial mass distribution must have been strongly aspherical, with a pole-to-equator contrast exceeding a factor of five.

In view of these kinematical complications, it is not surprising that shocks could play an extremely important role in the excitation of certain lines, particularly those of [NeV] as pointed out by Rowlands *et al.* (2). Shock effects may influence only a relatively small portion of emitting volumes but have an enormous influence on the intensities of the lines of high excitation, which originate in zones far hotter than predicted by any photoionization theory.

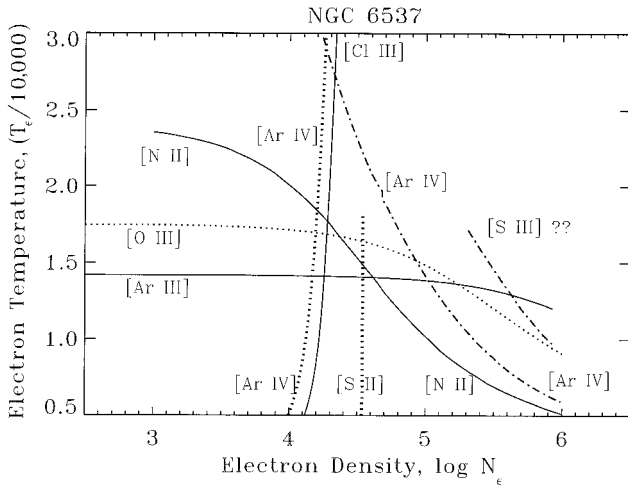
A strict photoionization theory is not adequate for NGC 6537 (2). Many years ago, Menzel and Aller (8) showed that, for a photoionized nebula of "normal" chemical composition, T_e could not much exceed 20,000 K, no matter how hot the exciting star. The [NeV] ions in NGC 6537 indicate a T_e of the order of 41,000 K (2), far in excess of that permitted in a pure photoionization scenario. The latter model may provide a good treatment for low stages of ionization and may prove useful for calculation of ionization correction factors.

One additional point needs emphasis. In NGC 6537, blobs and condensations lie below the limit of spatial resolution. In principle, their significance may be assessed with the aid of a diagnostic diagram (see Fig. 1). The usefulness of such diagrams is sensitive to the accuracy of the line intensities and atomic parameters, such as λ values and collision strengths. Of particular interest are the ions of p^3 configurations, most particularly those that produce lines of [OII], [NeIV], [SiII], [ClIII], and [ArIV]. By comparing intensities of both the auroral (or transauroral) and nebular transitions of these ions, we can get both T_e and N_e of the emitting layers. Recent improvements in observational data and theoretical data have greatly improved our insights.

In the following sections, we describe the ground-based and International Ultraviolet Explorer (IUE) data, the diagnostics, and attempt to draw some conclusions about the central star and nebular abundances. Table 1 gives the basic data taken largely from the catalogue by Acker *et al.* (9). Distance estimates have been made by Cahn *et al.* (10) and by Stanghellini *et al.* (11). Other data are discussed in the text.

Abbreviations: PN, planetary nebula; IUE, International Ultraviolet Explorer.

[‡]To whom reprint requests should be addressed. e-mail: aller@astro.ucla.edu; hyung@astro.ucla.edu or hyung@hanul.issa.re.kr; and feibelman@stars.gsfc.nasa.gov.

FIG. 1. Diagnostic diagram for NGC 6537: T_e vs. $\log N_e$.

The Observations

The observational and reduction procedures have been described by Hyung (12). A 640- μm entrance slit covers 2 pixels on the smaller (12- \times 12-mm chip) used in the 1992 observations. The effective resolution generally may be taken as 0.2 \AA (FWHM).

For the 1992 observations, we used a CCD chip with 800 \times 800 pixels, but, for the 1995 observations, we used a 2,048 \times 2048 chip. The 800 \times 800 pixel CCD did not cover the extent of the echelle spectrum, so several chip settings were needed, but the larger chip covers the entire spectrum. Table 2 gives the log of the Hamilton observations.

The interstellar extinction factor, C , can be found from the Balmer decrement, from the Paschen decrement (less reliably) and from a comparison of Paschen and Balmer lines arising from the same n . The intrinsic intensity values for the Paschen and Balmer lines are taken from Hummer and Storey (13). We find an extinction coefficient, $C = 1.80$, in good agreement with the Milne and Aller (14) measurements and compatible with the value $C = 1.95$ of Feibelman *et al.* (15).

Table 3 gives the Hamilton results: Successive columns give the measured wavelength, identified ion, multiplet number from Moore's Revised Multiplet Table (16, 17), the extinction parameter k_λ according to Seaton (18), the line intensity corrected for the interstellar extinction with $C = 1.80$, and the uncorrected intensity both on the scale $I(\text{H}\beta) = 100$. The measured wavelength is corrected for the nebular radial velocity, -10.1 km/sec, and for the effects of earth's motion about the sun.

The observations obtained with the IUE are listed in Table 4. The previous UV study of this PN used only one set of IUE observations. The short wavelength primary camera covers the wavelength region 1,159–2,000 \AA . The long wavelength redun-

Table 1. Some basic data for NGC 6537, PK 10 $^{\circ}$ 1

Basic data
$\alpha = 18^{\text{h}}05^{\text{m}}13^{\text{s}}.4$, $\delta = -19^{\circ}50'14''(2,000)$
Diameter = 10–34" $N_e \approx 20,000$ ml (see text)
$\log F(\text{H}\beta) = -11.40 \pm 0.03$ ($\text{erg}\cdot\text{cm}^{-2}\cdot\text{s}^{-1}$)
Radial Velocity = -16.0 ± 3.0 , -10.1 ± 1.0 (see text), $\text{km}\cdot\text{s}^{-1}$
Expansion velocity = 18.0 $\text{km}\cdot\text{s}^{-1}$ ([O III])
Central star: $m_B > 19.8$, $m_V > 18.8$
$T(\star) = 200,000$ K [SCS93]
Distance estimates (kiloparsecs): 0.90 [CKS91], 1.323[SCS93]

CKS91: Cahn, Kaler, and Stanghellini (10). SCS93: Stanghellini, Corradi, and Schwarz (11). Unless otherwise indicated, data are from Acker *et al.* (9)

Table 2. Ground-based observations

Set-up	Exposure, min	Observation Date, UT
121 (800)	60	June 18, 1992
127 (800)	5	June 18, 1992
124 (800)	60	June 19, 1992
125 (800)	60	June 19, 1992
125 (800)	3	June 19, 1992
126 (800)	60	June 19, 1992
123 (800)	60	June 19, 1992
127 (800)	60	June 19, 1992
– (2048)	165	July 3, 1995

See text and Hyung (12) for an explanation of six different set-up numbers, 125, 127, etc. . . . for 800 \times 800 charge-coupled device chip settings.

dant camera covers the range 1,850–3,300 \AA . The spectral resolution throughout the entire IUE range is 6–7 \AA . The entrance slit was an oval of 20 \times 23 arcsec dimension. Thus, because the optical region data were secured with an entrance slit of 4 arcsec and 640 microns wide (to preserve the purity of the spectrum), the two sets of observations referred to different areas of the PN, the IUE taking in the entire central region of this PN while the Hamilton echelle took in only a sample of this region. The effects of the differing apertures do not appear to be large. One advantage of the IUE was that it moved in a high, geostationary orbit, thus permitting very long exposures. The basic instrument is a Ritchie-Chretien telescope with a 45-cm primary mirror that feeds either of two echelle spectrographs. The detectors are a set of four identical secondary electron conduction vidicons that are coupled to proximity-focused UV-to-optical converters. The vidicons can integrate weak signals for hours, and, at the end of each exposure, their output signals are digitized by an on-board computer to 256 discrete levels and are read out at the end of each exposure.

Table 5 lists the UV lines observed. Successive columns give the measured wavelength, the identification, the value of the extinction coefficient, and the line intensity reduced to $I(\text{H}\beta) = 100$, corrected for interstellar extinction. In the next to the last column, we give the actual flux, and in the last column are remarks pertinent to the data.

Ionic Concentrations

Overview of Diagnostics. The following ions have been observed in the spectrum of NGC 6537: H, HeI, HeII, Cl?, CII, CII, CIII, [NI], [NII], NIII, NIII, NIV, NIV, NV, OI, [OI], OII, [OII], [OIII], OIII, ORV, ORV, [NeIII], [NeIV], [NeV], [MgI], [MgV], SII, SIII, SIV, [SII], [SIII], [SV], [ClII], [ClIV], [ArIII], [ArIV], [ArV], [KIV], [FeIII], [FeV], and [FeVII]. Note the richness of the IUE ionic spectra in this PN. We observe lines of HeI, HeII, Cl?, CII, CIII, CIV, NIII, NIV, NV, OI, [OII], OIV, [NeIII], [NeIV], [NeV], [MgV], SIII, SIV, and [ArIV].

Ionic Concentrations. Table 6 lists the diagnostic line ratios that are employed for a discussion of the plasma diagnostics. We successively list the ion, the line ratios that are employed, and the parameters that will determine N_e , T_e , or both.

The diagnostic diagram shows a fair amount of scatter, which is to be anticipated for an object with huge variations in T_e and N_e . The ratio of the nebular type transition in [NeIV] and [ClIII] lines suggest a density of $\approx 20,000/\text{cc}$ whereas the ratio of the first two nebular type transitions 6717/6739 of [SII] indicate a density of $\approx 31,700$ electrons/cc. The ratios of the auroral to nebular type transitions of [OIII] and [NII] would then suggest $T_e \approx 18,000$ K at $N_e \approx 10,000/\text{cc}$. For N and O++, we cannot find the densities without using infrared lines, for which we now have no data.

Thus, it is of special interest to get N_e and T_e for the same volume, as is possible for ions of the p^3 configuration, where

Table 3. Optical region line intensities in NGC 6537

$\lambda_{observed}$	λ_{lab}	Element	Mult.	k_λ	I(Ham)	F(Ham)	rms
3868.77	3868.71	[Ne III]	(1F)	0.228	107.2	41.69	20%
	3889.05	H I	H8				
3888.83	3888.65	He I	(2)	0.223	16.07	6.38	67%
3967.48	3967.41	[Ne III]	(1F)	0.203	33.97	14.62	4.8%
3970.11	3970.07	H I	H ϵ	0.203	7.908	3.41	31%
4068.61	4068.60	[S II]	(1F)	0.180	8.153	3.87	
4076.32	4076.35	[S II]	(1F)	0.178	1.996	0.95	
4097.42	4097.31	N III	(1)	0.173	4.639	2.26	
4101.71	4101.76	H I	H δ	0.172	14.12	6.92	66%
4103.40	4103.37	N III	(1)	0.172	2.188	1.07	
4338.64	4338.67	He II	(4-10)	0.129	2.809	1.64	19%
4340.44	4340.47	H I	H γ	0.129	41.68	24.43	17%
4363.19	4363.21	[O III]	(2F)	0.124	24.51	14.69	21%
4471.45	4471.48	He I	(14)	0.095	4.110	2.77	13%
4541.53	4541.59	He II	(9)	0.077	2.916	2.12	18%
4606.30	4606.60	Fe III	(3F)	0.061	1.276	0.99	
4634.11	4634.16	N III	(2)	0.054	2.415	1.93	20%
4638.28		line?		0.053	0.625	0.50	
4640.61	4640.64	N III	(2)	0.053	5.458	4.39	8.1%
4642.06	4641.81	N III	(2)	0.052	0.603	0.49	
4685.70	4685.68	He II	(3-4)	0.042	112.1	94.19	22%
4711.31	4711.34	[Ar IV]	(1F)	0.036	11.67	10.05	5.7%
4713.15	4713.14	He I	(12)	0.036	0.936	0.81	23%
4714.20	4714.25	[Ne IV]	(1F)	0.035	1.918	1.66	8.9%
4724.05	4724.15	[Ne IV]	(1F)	0.033	2.659	2.32	28%
4725.52	4725.62	[Ne IV]	(1F)	0.033	2.178	1.90	32%
4740.20	4740.20	[Ar IV]	(1F)	0.029	21.73	19.23	8.2%
4859.31	4859.32	He II	(4-8)	0	3.722	3.72	20%
4861.32	4861.33	H I	H β	0	100.0	100.0	9.9%
4921.92	4921.93	He I	(48)	-0.015	1.014	1.08	22%
4958.91	4958.92	[O III]	(1F)	-0.023	306.4	337.3	4.8%
5006.84	5006.84	[O III]	(1F)	-0.034	974.1	1122	5.8%
5015.68	5015.68	He I	(4)	-0.036	1.575	1.83	27%
5017.46	5017.48	†		-0.036	0.490	0.57	
5041.00	5041.06	Si II	(5)	-0.041	1.029	1.22	
	5056.35	Si II	(5)				
5056.02	5056.02	Si II	(5)	-0.045	0.754	0.91	
5191.74	5191.80	[Ar III]	(3F)	-0.073	0.394	0.53	13%
5197.98	5197.90	[N I]	(1F)	-0.074	1.255	1.71	
5200.34	5200.26	[N I]	(1F)	-0.074	0.591	0.81	
5309.26	5309.20	[Ca V]	-	-0.097	0.266	0.40	
	5412.00	[Fe III]	(1F)				
5411.53	5411.52	He II	(2)4-7	-0.118	8.461	13.80	6.3%
5461.13		line?		-0.128	1.102	1.87	53%
5517.51	5517.71	[Cl III]	(1F)	-0.139	0.385	0.69	23%
5537.82	5537.88	[Cl III]	(1F)	-0.143	0.916	1.66	8.5%
5679.56	5679.56	N II	(3)	-0.175	0.250	0.52	
5721.27	5721.10	[Fe VI]		-0.184	0.441	0.94	
5754.67	5754.64	[N II]	(3F)	-0.191	21.41	47.21	3.8%
5837.02	5837.06	He II	Pf32	-0.208	0.204	0.48	
5846.89	5846.65	He II	Pf31	-0.210	0.140	0.33	
5875.66	5875.67	He I	(11)	-0.216	13.01	31.84	8.2%
5953.03	5952.93	He II	Pf24	-0.229	0.158	0.41	
5977.00	5977.02	He II	Pf23	-0.233	0.225	0.59	5.9%
6004.63	6004.72	He II	Pf22	-0.238	0.184	0.49	1.8%
6036.98	6036.78	He II	Pf21	-0.243	0.296	0.81	29%
6074.21	6074.19	He II	Pf20(8)	-0.249	0.277	0.78	12%
6086.75	6086.90	[Cav, FevII]		-0.252	0.353	1.00	25%
6101.71	6101.80	[K IV]	(1F)	-0.254	0.875	2.51	9.7%
6118.24	6118.26	He II	Pf19	-0.257	0.216	0.63	10%
6170.69	6170.69	He II	Pf18	-0.265	0.257	0.77	16%
6228.27	6228.40	[K VI]		-0.274	0.261	0.81	20%
6233.88	6233.82	He II	Pf17(7)	-0.275	0.347	1.08	9.4%
6300.29	6300.30	[O I]	(1F)	-0.285	0.829	2.70	
6312.09	6312.10	[S III]	(3F)	-0.287	8.359	27.42	6.9%
6347.11	6347.09	Si II	(2)	-0.292	0.133	0.44	24%
6363.71	6363.78	[O I]	(1F)	-0.294	0.319	1.08	
6371.08	6371.36	Si II	(2)	-0.295	0.438	1.49	
6406.38	6406.38	He II	Pf15(7)	-0.301	0.518	1.80	11%
6435.00	6435.11	[Ar V]	(1F)	-0.305	8.661	30.62	9.6%
6478.36		N III	<i>CPM</i>	-0.311	0.186	0.68	
6500.28		Ar II	<i>CPM</i>	-0.314	0.181	0.67	
6513.19		line?		-0.316	0.116	0.43	
6516.29		[Mn V]	<i>CPM</i>	-0.316	0.100	0.37	

Table 3. Continued

$\lambda_{observed}$	λ_{lab}	Element	Mult.	k_λ	I(Ham)	F(Ham)	rms
	6527.23	[N II]					
6527.03	6527.10	He II	line?	-0.318	0.708	2.64	14%
6545.10				-0.320	0.165	0.62	
6548.11	6548.03	[N II]	(1F)	-0.321	111.35	420.7	6.1%
6560.07	6560.10	He II	(4-6)	-0.322	15.195	57.81	13%
6562.75	6562.82	H I	H α	-0.323	316.9	1208	4.8%
6568.65		line?		-0.324	0.076	0.29	
6580.92	6581.00	line?		-0.325	0.363	1.40	19%
6583.47	6583.45	[N II]	(1F)	-0.326	350.6	1352.07	8.6%
6600.57	6601.10	[Fe VII]	(1F)	-0.328	0.216	0.84	
6678.16	6678.15	He I	(46)	-0.338	3.181	12.93	10%
6683.19	6683.15	He II	Pf13(7)	-0.339	0.804	3.28	14%
6716.40	6716.47	[S II]	(2F)	-0.343	4.070	16.87	6.1%
6730.78	6730.85	[S II]	(2F)	-0.345	8.660	36.14	12%
6738.28	6739.4	[Sr II]?		-0.346	0.149	0.62	
6794.99	6795.00	[K IV]	(1F)	-0.352	0.238	1.02	
6890.91	6890.88	He II	Pf12(7)	-0.363	0.974	4.40	1.1%
7005.74	7005.70	[Ar V]	(1F)	-0.376	18.64	88.72	9.5%
7057.15		line?		-0.382	0.099	0.48	
7065.20	7065.28	He I	(10)	-0.383	6.587	32.21	9.6%
7135.78	7135.78	[Ar III]	(1F)	-0.391	29.99	151.4	7.3%
7170.70	7170.62	[Ar IV]	(2F)	-0.394	1.335	6.84	9.9%
7177.84	7177.50	He II	Pf11(6)	-0.395	0.513	2.64	44%
7237.63	7237.54	[Ar IV]	(2F)	-0.401	1.415	7.46	2.1%
7262.90	7262.96	[Ar IV]	(2F)	-0.404	1.122	5.98	21%
7281.35	7281.35	He I	(45)	-0.406	0.729	3.92	5.4%
7320.00	7319.80	[O II]	(2F)	-0.410	8.213	44.87	0.6%
7330.20	7330.70	[O II]	(2F)	-0.411	6.913	37.93	5.4%
7458.38		line?		-0.423	0.079	0.46	
7499.89	7499.84	He I	(1/8)	-0.428	0.052	0.31	
7530.38	7530.83	[Cl IV]	(1F)	-0.430	1.184	7.05	0.5%
7582.12		line?		-0.435	0.200	1.21	
7592.69	7592.74	He II	Pf10(6)	-0.436	1.890	11.53	12.1%
7618.50	7618.5	N V	(14)	-0.439	0.409	2.52	4.0%
7703.32	7703.3	N IV	(23)	-0.447	0.269	1.71	58%
7712.71	7713.3	O IV?	(21)	-0.448	0.164	1.05	11%
7726.14	7726.20	C IV	(8,01)	-0.449	0.099	0.64	22%
7751.11	7751.43	[Ar III]	(1F)	-0.451	8.633	55.98	17%
7816.37	7816.16	He I	(69)	-0.457	0.119	0.79	
8045.66	8046.27	[Cl IV]?	(1F)	-0.477	2.564	18.49	9.3%
8192.23		line?		-0.489	0.138	1.04	
8196.51	8196.48	C III	(43)	-0.489	0.165	1.26	17%
8236.77	8236.78	He II	Pf9	-0.492	2.759	21.23	1.3%
8281.15	8281.12	H I*	P31	-0.496	0.112	0.87	
8286.32	8286.43	H I	P30	-0.496	0.134	1.04	12%
8292.05	8292.31	H I	P29	-0.497	0.122	0.95	43%
8298.79	8298.84	H I	P28	-0.497	0.111	0.87	34%
8306.67	8306.12	H I*	P27	-0.498	0.177	1.39	
8314.17	8314.26	H I	P26	-0.498	0.155	1.22	
8315.36	8315.10	C III	5g-6h	-0.499	0.170	1.35	
8323.59	8323.43	H I	P25	-0.499	0.180	1.43	31%
8333.86	8333.78	H I	P24	-0.500	0.191	1.52	
8333.93	8333.78	H I	P24	-0.500	0.202	1.60	
8345.56	8345.55	H I	P23	-0.502	0.205	1.64	6.1%
8359.02	8359.01	H I	P22	-0.504	0.170	1.37	12%
8374.53	8374.48	H I	P21	-0.506	0.163	1.33	15%
8379.66	8379.60	He II	(6-41)	-0.507	0.040	0.32	
8386.56		†		-0.508	0.063	0.52	
8392.33	8392.40	H I	P20	-0.509	0.213	1.76	37%
8413.29	8413.32	H I	P19	-0.512	0.226	1.89	17%
8434.36	8433.85	[Cl III]	(3F)	-0.516	0.191	1.62	
8437.94	8437.96	H I	P18	-0.516	0.272	2.31	31%
8446.65	8446.48	O I	(4)	-0.517	0.052	0.45	
8467.27	8467.26	H I	P17	-0.521	0.354	3.06	18%
	8481.16	[Cl III]	(3F)				
8480.70	8480.73	He I		-0.523	0.120	1.05	
8502.45	8502.49	H I	P16	-0.526	0.331	2.92	32%
8545.37	8545.38	H I	P15	-0.532	0.436	3.96	9.3%
8567.03	8566.90	He II	(6-29)	-0.536	0.067	0.62	
8578.90	8578.70	[Cl II]	(1F)	-0.537	0.296	2.75	1.4%
8598.34	8598.39	H I	P14	-0.540	0.590	5.53	17%
	8662.00	He I	(10/14)				
8661.54	8661.40	He II	(6-26)	-0.549	0.135	1.31	

(Table continues on the opposite page.)

Table 3. Continued

$\lambda_{observed}$	λ_{lab}	Element	Mult.	k_λ	I(Ham)	F(Ham)	rms
8665.00	8665.02	H I	P13	-0.550	0.883	8.63	19%
8750.50	8750.48	H I	P12	-0.562	0.942	9.68	1.0%
8799.00	8798.90	He II	(6-23)	-0.569	0.078	0.83	
8850.17	8849.0	He I?	(3/9)	-0.576	0.135	1.47	
8862.55	8862.79	H I	P11	-0.578	1.953	21.43	51%
9010.95	9011.20	He II	(6-20)	-0.598	0.154	1.84	
9014.86	9014.91	H I	P10	-0.599	1.797	21.48	23%
9068.66	9068.90	[S III]	(1F)	-0.606	21.16	260.6	19%
9076.85		†		-0.607	0.221	2.74	
9210.44	9210.28	He I	(83), 6/9	-0.612	0.086	1.08	
9223.90	9223.0	N v?		-0.612	0.631	7.98	
9228.94	9229.02	H I	P9	-0.612	2.108	26.67	13%
9367.63	9367.1	He II	(6-17)	-0.616	0.143	1.83	
9463.44	9463.57	He I	(1/5)	-0.618	0.240	3.10	
9526.29	9526.00	He I	(6/8)	-0.620	0.162	2.12	
9530.93	9531.00	[S III]	(1F)	-0.620	98.28	1282	6.5%
9542.39	9542.00	He II	(6-16)	-0.620	0.234	3.05	44%
9545.98	9545.97	H I*	P8	-0.620	0.893	11.67	25%
9547.79		line?		-0.620	3.294	43.05	
9624.13	9625.64	He I??	(10/8)	-0.622	0.121	1.59	
9705.22	9705.9	C III		-0.624	0.120	1.59	
9807.72		line?		-0.626	0.163	2.18	
9912.87		line?		-0.629	0.306	4.14	
10045.57	10045.20	He II	(6-14)	-0.631	0.292	4.00	25%
10049.32	10049.38	H I	P7	-0.632	3.796	52.00	16%
10123.89	10123.61	He II	(4-5)	-0.633	6.318	87.00	83%
10286.78	10296.5	[S II]??	(3F)	-0.636	1.951	27.29	

Extinction corrected with $C = 1.80$ (see text). For the identification, see Hyung and Aller (25) and references therein cited. See Péquignot and Baluteau (26) for [Kr IV] 5867.8?

*, Lines affected by atmosphere.

?, Unlikely or doubtful identification.

†, These unidentified lines are seen in other PN, i.e., IC 4997, NGC 7027, and NGC 7662.

^{CPM}, Identification by Cuesta, Phillips, and Mampaso (7), but other lines, such as 6396 [Mn V], 6463/67 N III, and 6853 [Mn VI], are not seen!

we can compare the nebular-type ratios with the auroral/nebular ratio. Thus, in [Ar IV], we may compare the nebular-type lines 4711 and 4740 with the auroral type transitions 7171, 7237, and 7263. That is, we plot $\{I(7171) + I(7238) + I(7263)\}/\{I(4711) + I(4740)\}$ against the nebular line ratio $\{I(4711)/I(4740)\}$. The first ratio depends on both T_e and N_e , but, at nebular densities, the latter depends exclusively on the density. We usually get a good fix on N_e in the layer emitting the p^3 lines in question. Aside from observational errors and uncertainties in theoretical ratios, there are also the N_e fluctuations along the line of sight, but, perhaps, the largest error accrues from uncertainties in the interstellar extinction, which can be troublesome when space absorption is large.

Favorite ions have long been [O II] and [S II]. In NGC 6537, [O II] is not useful because of heavy interstellar extinction, but the [S II] transauroral type 4068 and 4076 lines and the nebular type 6717 and 6730 indicate $N_e \approx 31,700/\text{cc}$ and $T_e \approx 6,500$ K. Thus, the [S II] radiation appears to originate in clumps considerably denser and cooler than those responsible for the [O II] radiation. Lines of ionized neon are particularly valuable in assessing the highly excited regions. Rowlands *et al.* (2) combined data from the infrared 14.4- and 24- μm infrared lines with the 3,426-Å line to get $\log N_e \approx 4.07$ and $T_e \approx 41,000$,

Table 4. IUE observing log for NGC 6537

Spectrum	Dispersion	Date	Exposure, min	Notes
SWP 24281	Low	June 23, 1984	210	On star
SWP 35967	Low	April 9, 1989	220	On star
LWR 15324	Low	April 8, 1989	240	On star

The fluxes are taken through the large IUE entrance aperture, 10×23 arcsec² centered on star. SWP, short wavelength primary camera; LWR, long wavelength redundant camera.

Table 5. Observed IUE emission lines from two co-added short wavelength primary camera and single long wavelength redundant camera spectra

$\lambda_{observed}$	Ion	k_λ	I(IUE)	Flux*	Notes
1238.45	N V	1.638	582	2.55	Doublet
1379.52	O v?	1.339	49.7	0.77	
1402.50	O IV]1397-1407, Si IV	1.306	9.03	0.16:	Very weak
1484.79	N IV]1483/87	1.231	163	3.95	Doublet
1548.79	C IV 1548/50	1.184	313	9.23	Doublet
1577.86	[Ne v]?	1.166	37.5	1.19	
1597.84	[Ne IV]?	1.155	36.8	1.22	
1641.14	He II	1.136	140	5.04	P Cyg?
1663.63	O III]	1.128	105	3.91	Doublet
1734.07	N III?	1.118	40.7	1.57	
1749.48	N III]	1.119	105	4.02	Quintet
1835.14	?	1.152	44.7	1.50	
1889.67	Si III]1882/92	1.203	54.9	1.49	
1908.20	C III]1907/09	1.227	131	3.22	Doublet
2423.27	[Ne IV]2423/5	1.118	186	7.20	Doublet
3130.53	O III	0.455	38.8	23.44	Bowen line
3200.17	He II 3203	0.426	13.8	9.42	

Colon means estimated errors are large, $\pm 40\%$, others $\pm 15\%$. The UV line intensities in column 4 are given based on the scale of $I(H\beta) = 100$ (with the interstellar extinction corrections, $C = 1.80$).

*The fluxes are in units of 10^{-14} ergs $\cdot\text{cm}^{-2}\cdot\text{s}^{-1}$.

which is far above any T_e suggested by a photoionization model. A yet higher T_e occurs in NCG 6302!

For [Ne IV], data on the separate components of the 2,423 pair is not yet available. We assumed $N_e = 15,000/\text{cc}$ and used the 4711/2432 and the 4749/2423 ratio to get $T_e = 30,000$ K, a temperature still higher than what is permitted by photoionization models.

Despite uncertainties in the T_e determination, the evidence points to a smooth rise from near 13,000 or 15,000 for O II and N II to $T_e \approx 41,000$ for ions like Ne V, which require 97 eV.

Table 7 gives the fractional ionic concentrations obtained on the basis of an empirical temperature calibration. For each ion, we list the lines used, the adopted value of T_e , the line intensity, and, finally, $N(\text{ion})/N(\text{H}^+)$. The electron density is taken as $\approx 20,000$, except for the [S II] zone.

Abundances

Table 8 gives for each element the sum of the ionic abundances with respect to ionized H. The third column gives the ionization correction factor. These are taken from the best photoionization model and are subject to large uncertainties for elements represented by only one or two ionization stages, such as Si, K, or Ca.

Table 9 compares three determinations of abundances in NGC 6537 with mean values for PN proposed by Kingsburgh

Table 6. Diagnostic line ratios

Ion	Lines	Ratio	Determines	Notes
[N I]	I(λ5200)/I(λ5198)	0.47	N_e	N/A?
[N II]	I(λ6548 + λ6583)/I(λ5755*)	21.6	T_e	
[O III]	I(λ4959 + λ5007)/I(λ4363)	52.2	T_e	
[S II]	I(λ6716‡)/I(λ6731)	0.45	N_e	
[S III]	I(λ9069 + λ9531†)/I(λ6312)	14.3	T_e	
[Ar III]	I(λ7136 + λ7751)/I(λ5191*)	84.7	T_e	
[Ar IV]	I(λ4711)/I(λ4740)§	0.54	N_e	
[Ar IV]	I(λ4711 + 40)/I(λ7170)	16.7	N_e, T_e	
[Cl III]	I(λ5538)/I(λ5518)	2.18	N_e	

N/A?, Useless because of its poor measurement.

*Relatively weak line.

†Affected by atmospheric extinction.

‡Affected by H α drip (correction was made).

§See Keenan *et al.* (19).

Table 7. Fractional ionic concentration for NGC 6537

Ion	Lines	T_e	I_{corr}	$N(ion)$
				$N(H^+)$
He I	6678	17000	3.18	7.37(-2)
	4471		4.11	8.96(-2)
	5876		13.0	6.00(-2)
He II	4686	20100	112	1.00(-1)?
	5412		8.46	5.70(-2)
C III	1907/9	18000	131	9.70(-2)
C IV	1545/51	23000	313	3.30(-6)
N I	5198, 5200	6000	1.85	6.50(-5)
N II	6548/84,5755	12500	483	4.84(-5)
N III	1747-54	18000	105	3.02(-5)
N IV	1483/86	24000	163	9.82(-6)
N V	1239/43	34000	582	2.87(-6)
O I	6300/63	10800	1.15	9.93(-7)
O II	7319/30	12700	15.1	2.62(-5)
O III	4959, 5007, 4363	17700	1305	7.92(-5)
	1666-		105	9.94(-5)
O IV	1397-1407	25000	9.03	1.86(-6)
Ne III	3868, 3967	15900	141	1.87(-5)
Ne IV	4724/6,4714	30000	6.76	4.40(-6)
	3345/3426		681*	1.33(-5)
Ne V	1575	40000	37.5	1.49(-5)
	6717/31,4068/76		6200	22.9
S II	6312/9069/9532	12000	121.8	3.08(-6)
Cl II	8580	8600	0.3†	4.10(-8)
Cl III	5517/37	14000	1.30	4.97(-8)
Cl IV	7530/8045	23000	3.75	5.59(-8)
Ar III	7135, 7751, 5192	14200	39.02	1.26(-6)
Ar IV	4711/40,7263/40+	20000	37.27	7.02(-7)
Ar V	6435,7005	25000	27.30	5.57(-7)
Si III	1882/92	18300	54.9	8.16(-7)
K IV	6102	25000	0.875	3.99(-8)
Ca V	5309	32000	0.266	1.79(-8)

X(-Y) implies $X \times 10^{-Y}$. $N_e = 20,000$.

*From Feibelman, Aller, Keyes, and Czyzak (15).

†Discarded because of its uncertain intensity.

and Barlow (22) and with solar values proposed by Grevesse and Noels (23). Feibelman *et al.* (15) observed the bright central core of NGC 6537 with an image scanner. Perinotto and Corradi (24) selected three positions of the nebular image (see their Figs. 1 and 3). They used optical region data only. Perhaps, in view of the uncertainties involved, the discordances are not surprising.

The larger helium abundance (15) may be more nearly correct for this type I PN. Carbon is less abundant than in the sun or a typical PN. Possibly, it has largely processed into N in the CNO cycle. N is uncertain and merits intensive further

Table 8. Elemental abundances of NGC 6537

Element	$\sum \frac{N(ion)1}{N(H^+)}$	ICF	$\frac{N(element)}{N(H^+)}$
He I, II	0.131	-	0.131
C III, IV	1.30(-5)	1.600	2.08(-5)
N II, III, IV, V	9.13(-5)	1.087	9.92(-4)
O II, III, IV	1.17(-4)	1.215	1.42(-4)
Ne III, IV, V	3.72(-4)	1.292	4.81(-5)
S II, III	1.00(-5)	2.994	2.99(-5)
Cl II, III, IV	1.47(-7)	1.894	2.78(-7)
Ar III, IV, V	2.52(-6)	1.548	4.00(-6)
K IV	2.99(-8)	3.010	1.20(-7)
Ca V	1.79(-8)	7.143	1.28(-7)
Si III	8.16(-7)	10.89	8.89(-6)

X1,X2(-Y) implies $X1 \times 10^{-Y}$, $X2 \times 10^{-Y}$. ICF, ionization correction factor.

Table 9. Comparison of abundances

Element	NGC 6537			Sun†
	OUR	FAKC	KB*	
He	0.131	0.189	0.11	0.1
C	2.08(-5)	4.0(-5)	6.48(-4)	3.55(-4)
N	9.92(-5)	8.9(-4)	1.40(-4)	9.33(-5)
O	1.42(-4)	1.7(-4)	4.93(-4)	7.41(-4)
Ne	4.81(-5):		1.25(-4)	1.17(-4)
S	2.99(-5)		8.08(-6)	1.62(-5)
Ar	4.00(-6)		2.42(-6)	3.98(-6)
Cl	2.78(-7)		1.66(-7)‡	3.88(-7)
Ca	1.28(-7)			2.29(-6)
K	1.20(-7)			1.35(-7)
Si	8.89(-6)			3.55(-5)

X(-Y) implies $X \times 10^{-Y}$. OUR, The current estimates based on the model; FAKC, Feibelman *et al.* (15). ; Uncertainty estimated $\geq 50\%$.

*Average nebular abundances by Kingsburgh and Barlow (22).

†Grevesse and Noels (23).

‡Average abundances by Aller and Czyzak (27).

study. Discordances for O, Ne, and Ar are smaller. Sulfur presents a problem. The [SII] emission arises in dense, cool blobs; the pertinent ionization correction factors seem poorly determined. Si, K, and Ca, observed only in one ionization state, are very uncertain.

NGC 6537 shows no extreme abundance anomaly with respect to the sun, with the possible exception of O, which may have been decreased by hot bottom burning, and, perhaps, calcium and silicon that are tied up in grains.

Concluding Remarks

NGC 6537 is one of the most remarkable high excitation PN known. It is an unusually high excitation object, showing electron temperatures as high as 40,000 K in the [Nev] region and as low as 6,500 K in the [SII] filaments. Excitation by shock waves is prominent in this kinematically active nebula, so that a pure photoionization model, which seems adequate for many planetaries, fails here. The importance of high dispersion observations and accurate atomic parameters (19-21) so that good plasma diagnostics can be obtained is amply demonstrated. This is very true for nebulae where the structural detail is not resolved.

Despite a fair amount of observational data (more than for some PN believed to be amenable to good abundance analyses), NGC 6537 presents formidable challenges. Further infrared data are urgently needed, not only to improve diagnostics, but because the effects of space absorption are less severe here.

W.A.F. is a guest observer with the IUE satellite, which is sponsored and operated by the National Aeronautics and Space Administration, by the European Space Agency, and by the Science and Engineering Council of the U.K. We are grateful for a grant from the STSI, National Aeronautics and Space Administration support for the IUE observations, and support from the University of California at Los Angeles research grants committee.

1. Ashley, M. C. B. & Hyland, A. R. (1988) *Astrophys. J.* **331**, 532-538.
2. Rowlands, N., Houck, J. R. & Herter, E. (1994) *Astrophys. J.* **427**, 867-875.
3. Meaburn, J. & Walsh, J. R. (1965) *Mon. Not. R. Astron. Soc.* **215**, 761-771.
4. Peimbert, M. & Torres-Peimbert, S. (1983) in *Planetary Nebulae, International Astronomical Union Symposium No. 103*, ed. Flower, (Kluwer, Dordrecht, The Netherlands), pp. 233-242.
5. Corradi, R. L. M. & Shwarz, H. (1993) *Astron. Astrophys.* **269**, 452-468.
6. Phillips, J. P. & Mampaso, L. (1988) *Astron. Astrophys.* **190**, 237-259.

7. Cuesta, L., Phillips, J. P. & Mampaso, A. (1995) *Astron. Astrophys.* **304**, 475–490.
8. Menzel, D. H. & Aller, L. H. (1941) *Astrophys. J.* **91**, 30–36.
9. Acker, A., Ochsenbein, F., Stenholm, B., Tylenda, R., Marcout, J. & Schohn, C. (1992) *Sirasbourg-ESO Catalogue of Galactic Planetary Nebulae* (European Southern Observatory, Garching bei Munchen, Germany).
10. Cahn, J. H., Kaler, J. B. & Stanghellini, L. (1992) *Astron. Astrophys. Suppl.* **94**, 399–452.
11. Stanghellini, L., Corradi, R. L. M. & Schwarz, H. E. (1993) *Astron. Astrophys.* **276**, 463–469.
12. Hyung, S. (1994) *Astrophys. J. Suppl.* **90**, 119–148.
13. Hummer, D. G. & Storey, P. J. (1987) *Mon. Not. R. Astron. Soc.* **224**, 801–820.
14. Milne, D. & Aller, L. H. (1975) *Astron. Astrophys. Suppl.* **38**, 183–196.
15. Feibelman, W. A., Aller, L. H., Keyes, C. D. & Czyzak, S. J. (1985) *Proc. Natl. Acad. Sci. USA* **83**, 2202–2206.
16. Moore, C. E. (1974) *A Multiplet Table of Astrophys. Interest, National Bureau of Standards, No. 40* (National Bureau of Standards, Washington, DC).
17. Moore, C. E. (1993) *Table of Spectra of H, C, N & O: Atoms and Ions*, ed. Gallagher, J. W., (CRC, Boca Raton, FL).
18. Seaton, M. J. (1979) *Mon. Not. R. Astron. Soc.* **187**, 73P–76P.
19. Keenan, F. A., McKenna, F., Bell, K. L., Aller, L. H., Ramsbottom, K. & Wikstead, A. W. W (1997) *Astrophys. J.* **487**, 457–462.
20. Keenan, F. A., Aller, L. H., Hyung, S., McKenna, F. & Ramsbottom, K. (1996) *Mon. Not. R. Astron. Soc.* **291**, 1073–1080.
21. Keenan, F. A., Aller, L. H., Hyung, S., Feibelman, W. A., Bell, K. L., McKenna, F. & Ramsbottom, K. (1998) *Mon. Not. R. Astron. Soc.* **295**, 683–690.
22. Kingsburgh, R. L. & Barlow, M. J. (1992) *Mon. Not. R. Astron. Soc.* **271**, 257–294.
23. Grevesse, N. & Noels, A. (1993) in *Origin and Evolution of the Elements*, ed. Prantzos, N., Vangioni-Flam, E. & Casse, M. (Cambridge Univ. Press, Cambridge, U.K.), pp. 15–20.
24. Perinotto, M. & Corradi, R. L. M. (1998) *Astron. Astrophys.* **332**, 721–731.
25. Hyung, S. & Aller, L. H. (1997) *Mon. Not. R. Astron. Soc.* **293**, 71.
26. Péquignot, D. & Baluteau, J. P. (1994) *Astron. Astrophys.* **283**, 593.
27. Aller, L. H. & Czyzak, S. J. (1983) *Astrophys. J.* **51**, 211.